TR - H - 178

Time-domain Simulations of Sound Production in an Organ Flue Pipe

Seiji Adachi

1995. 12. 11

ATR人間情報通信研究所

〒619-02　京都府相楽郡精華町光台2-2　☎ 0774-95-1011

ATR Human Information Processing Research Laboratories
2-2, Hikaridai, Seika-cho, Soraku-gun, Kyoto 619-02 Japan
Telephone: +81-774-95-1011
Facsimile: +81-774-95-1008

Time-Domain Simulations of Sound Production in an Organ Flue Pipe

Seiji ADACHI

ATR Human Information Processing Research Laboratories

Due to the difficulty in treating jet behavior, a general agreement on the sound production of flue instruments has not yet been obtained. This paper examines jet deflection models presented by several authors by means of the time-domain approach. Simulations of an organ flue pipe where the blowing pressure is changed as a parameter are carried out. The results are compared with those obtained in experiments.

1 Introduction

Flue instruments such as a flute and a recorder are also called air-reed instruments. This is due to the analogy of an air jet emerging from the flue slit and swaying transversely to its direction of travel with a vibrating reed of the other type of the woodwind instruments. The jet supplies a pulsating airflow, which drives the sound field in the pipe. Conversely, the sound field interacts with the jet at the mouth and controls jet deflection. Therefore, the sound production forms a feedback loop.

The organ provides a major group of pipes called flue pipes. To cover a wide range of sound timbre and register, there are a variety of flue pipes having different shapes and dimensions. However, each pipe produces sound functionally in the same way as flue instruments An organ flue pipe has a relatively simple acoustic structure compared with other flue instruments, because it has no tone holes. Therefore, a flue pipe is often selected as representative of the flue instrument family.

From research done over the past hundred years, a general understanding of the sound production of flue instruments as a feedback system has been obtained. Simple theories give reasonable agreement with experiments on level and spectrum of the sound generated in an instrument. However, we have not yet obtained a satisfactory understanding of the interaction between air jet and sound field, which is crucial to this feedback system. It seems formidably difficult to theoretically derive jet behavior traveling through the mouth in the presence of sound field from the first principle of the fluid dynamics.

In this circumstance, we should rely on discussions of idealized situations, hypotheses and experimental data to model jet behavior. Currently, there are three plausible models along this line. In these models, different physical quantities are assumed as the sound field driving the air jet.

Fletcher and Thwaites proposed their model, where acoustic particle displacement drives the jet.[2] This model assumes that acoustic displacement at the flue slit exit causes an infinitesimal disturbance of the jet. The disturbance propagates and grows due to jet instability while the jet is traveling through the mouth. This explains how jet deflection occurs. The model proposed by Coltman[3] assumes acoustic particle velocity as the jet driving source. In this model, jet center position (which gives the maximum of the velocity profile in the direction of jet thickness) becomes a functional of acoustic velocity while the jet is passing through the

mouth. The model by Yoshikawa and Saneyoshi[4] assumes that acoustic pressure gradient in the direction of jet thickness drives the jet deflection.

Coltman examined these three models, by carrying two experiments,[5] which indicate somewhat contradictory results. Therefore, no definite conclusion of which model replicates actual jet behavior most precisely could be drawn out from his experiments.

Along with the progress of computational power, there is an attempt to examine jet behavior using a numerical method directly to solve fluid dynamical equations.[6] There is also an experiment to visualize the jet at the level of vortex shedding.[7] However, these researches has not addressed modeling of jet deflection.

The aim of this paper is to compare performances of the three jet deflection models using time-domain simulations of a pipe. The fundamental frequency and spectrum of simulated sound as functions of blowing pressure are obtained. These are compared with results obtained by the experiment.

The next section reviews the jet deflection models. Section 3 discusses the velocity profile of the air jet. In Sec. 4, we obtain time-domain representations of the models. The self-excited system of the sound production is described and results of the simulation with this system are presented in Sec. 5. Section 6 concludes this paper.

2 Jet deflection models

An air jet emerging from a flue slit impinges on the edge after traveling through the mouth (Fig. 1). While traveling, the air jet is displaced in the direction of jet thickness, i.e., vertical direction in Fig. 1, due to the presence of sound field at the mouth. Jet displacement is denoted by the center position of the jet thickness $\xi(x,t)$, where x is the horizontal distance from the exit of the flue slit and t is time. The displacement $\xi(x,t)$ is measured vertically from the center line of flue slit thickness. Positive displacement is

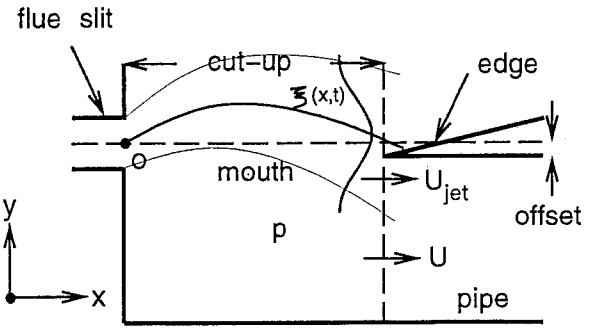

Figure 1: Schematic diagram of flue slit, mouth and edge of an organ flue pipe

defined to be toward the outside of the instrument, i.e., the upper direction.

The actual jet spreads transversely and gradually decelerates while passing through the mouth. These effects are considered in Sec. 3; we tentatively assume that the jet does not spread and that it travels with a constant velocity V_{jet}.

Depending on which sound field is assumed to affect the jet displacement $\xi(x,t)$,

(a) acoustic displacement $X(t)$,

(b) acoustic particle velocity $v(t)$, or

(c) pressure gradient $\Delta p(t)$,

three different jet deflection models are proposed. These sound fields are assumed to be uniform along the horizontal distance at the mouth, from the flue slit exit to the edge, and only depend on time t. Positive directions of $X(t)$ and $v(t)$ are defined to be toward the outside of the instrument in the same way as the definition of $\xi(x,t)$. Based on physical intuition, $\Delta p(t)$ is defined to be positive if pressure decreases toward the outside of the instrument.

2.1 Negative acoustic displacement model

This model[2] assumes (a) acoustic displacement $X(t)$ as the jet driving source; the ratio

of jet displacement to acoustic displacement is given by

$$\frac{\xi_\omega(x)}{X_\omega} = 1 - \cosh \mu x \; e^{-i\omega \frac{x}{V_{\text{phase}}}}, \qquad (1)$$

where ω is angular frequency and $\xi_\omega(x)$ and X_ω denote the frequency components of $\xi(x,t)$ and $X(t)$, respectively. Model parameters μ and V_{phase} in Eq. (1) are the amplification coefficient and phase (propagation) velocity of the jet displacement, respectively. The first term of the r.h.s. in Eq. (1) indicates that the jet transversely moves as a lump with the displacement of the air $X(t)$. The second term describes how a small disturbance of the jet $-X$ at $x = 0$ propagates and grows due to jet instability. Therefore, this model is called the negative acoustic displacement model.

The model assumes an exponential increase of jet disturbance. However, it is actually observed only for an infinitesimal displacement, and gives way to a linear increase of the finite one. Hereafter, we consider only the first two terms of the expansion of cosh.

Generally, amplification coefficient μ and phase velocity V_{phase} depend on frequency ω. The dependence was determined by the theory of jet instability in the case of inviscid flow, and also confirmed by experiments. Functional forms and their approximations by analytic functions are discussed in Sec. 4.1.

The jet displacement $\xi_\omega(x,t)$ can be calculated immediately from Eq. (1) for the acoustic displacement X oscillating sinusoidally. The solid line in Fig. (2) denotes $\xi_\omega(x,t)$ derived in this model at the reference time when the X is most negatively displaced. At this moment, acoustic particle velocity v is zero changing negative to positive, and the pressure gradient Δp reaches the maximum.

2.2 Acoustic particle velocity model

This model[3] assumes (b) acoustic particle velocity as the driving source. The ratio of

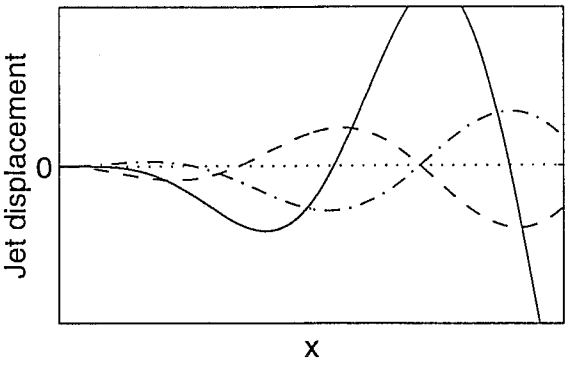

Figure 2: Jet displacement $\xi(x)$ at the time of peak negative acoustic displacement (the furthest inside the instrument). Solid line depicts $\xi(x)$ for (a) the negative acoustic displacement drive model, dashed line depicts $\xi(x)$ for (b) the acoustic velocity drive model, and dash-dot line depicts $\xi(x)$ for (c) the pressure gradient drive model.

$\xi_\omega(x)$ to v_ω is given by

$$\frac{\xi_\omega(x)}{v_\omega} = T \; e^{-i\omega T}, \qquad (2)$$

where the delay time of interaction T is assumed to be $T = x/V_{\text{jet}}$.

The dashed line in Fig. 2 denotes jet displacement $\xi_\omega(x,t)$ at the reference time based on this model.

2.3 Pressure gradient model

In this model, the pressure gradient Δp transverse to the direction of jet travel becomes the driving source.[4] Applying the equation of motion to an infinitesimal volume element flowing with the jet, we obtain the jet displacement $\xi_\omega(x)$. The ratio of $\xi_\omega(x)$ to Δp_ω becomes

$$\frac{\xi_\omega(x)}{\Delta p_\omega} = \frac{1}{\rho\omega^2}\left(-1 + (1 + i\omega T)\; e^{-i\omega T}\right), \qquad (3)$$

where ρ is the air density and $T = x/V_{\text{jet}}$.

The dash-dot line in Fig. 2 depicts $\xi_\omega(x,t)$ at the reference time in the model.

3 Velocity profile of the jet

In the mouth, the jet has a bell-shape velocity profile in the direction of jet thickness. We assume the profile $V(y) = V_c \mathrm{sech}^2 y/b$, where y is the distance from the jet center line, V_c is the jet center velocity and b is the half-thickness of the jet. We assume that the jet has a uniform velocity profile in the flue slit.

While traveling through the mouth, the jet blends into the surrounding air. Therefore, the tophat shape of the velocity profile at the flue exit gives way to the bell shape profile in the mouth. Moreover, as the jet travels, the half-thickness b increases and the center velocity V_c decreases. Assuming momentum conservation and a constant spreading angle ϕ of the jet, we have

$$b(x) = b_0 + x\tan\phi, \quad (4)$$

$$V_c(x) = V_0\sqrt{b_0/b(x)}, \quad (5)$$

where b_0 and V_0 are the jet half-thickness and the center velocity at the flue exit, respectively. These are given by $b_0 = 0.75h$ and $V_0 = \sqrt{2p_0/\rho}$, with flue slit thickness h and blowing pressure p_0.

The time needed for the center of the jet to travel from the flue exit to the edge can be calculated as

$$\int_0^l \frac{dx}{V_c(x)} \equiv \frac{l}{\bar{V}_c}, \quad (6)$$

with cutup length l. Equation (6) can be considered the definition of the "mean" center velocity $\bar{V}_c$.

Due to the bell shape velocity profile of the jet, the relation between the "mean" center velocity $\bar{V}_c$ and the jet velocity V_{jet} introduced in the previous section is ambiguous. We thus introduce a factor $\gamma < 1$ that is defined by

$$V_{\mathrm{jet}} = \gamma\bar{V}_c. \quad (7)$$

This factor γ is used as a parameter of the simulation.

When the jet displacement $\xi(l,t)$ at the edge is known, we can easily calculate the jet volume flow U_{jet} into the pipe by integrating the velocity profile within the inside of the instrument as follows:

$$U_{\mathrm{jet}} = Wb(l)V_c(l)\left(1 - \tanh\frac{\xi(l) - h_{\mathrm{off}}}{b(l)}\right), \quad (8)$$

where W is mouth width and h_{off} is offset of the edge position from the center line of the flue slit (a positive value means toward the upper direction).

4 Time-domain representation

4.1 Negative acoustic displacement model

For a technical reason, it is convenient to use acoustic particle velocity $v(t)$ instead of acoustic velocity $X(t)$ as a variable in the simulation described in the next section. Therefore, we modify Eq. (1) with the velocity amplitude $v_\omega = i\omega X_\omega$ as follows:

$$\frac{\xi_\omega(x)}{v_\omega} = \frac{1}{i\omega}\left[1 - \left(1 + \frac{1}{2}(\mu x)^2\right)e^{-i\omega\frac{x}{V_{\mathrm{phase}}}}\right]. \quad (9)$$

The expansion $\cosh\theta = 1 + \theta^2/2$ up to the second term as was described in Sec. 2.1 is used.

It is necessary to find the frequency dependence of amplification coefficient μ and phase velocity V_{phase} to obtain a definite time-domain representation.

In Ref. [2], discussions on instability of the inviscid flow yield the following amplification coefficient:

$$\mu b = 0.74\left(1 - e^{-3kb}\right) - 0.37kb \quad (10)$$

for $0.1 \le kb \le 2$, where $k \equiv \omega/V_{\mathrm{phase}}$ is the wave number and b is the jet half-thickness. It is shown that this frequency dependence gives qualitative agreement with an experiment.[8] The solid line in Fig. 3 depicts the functional form of μ.

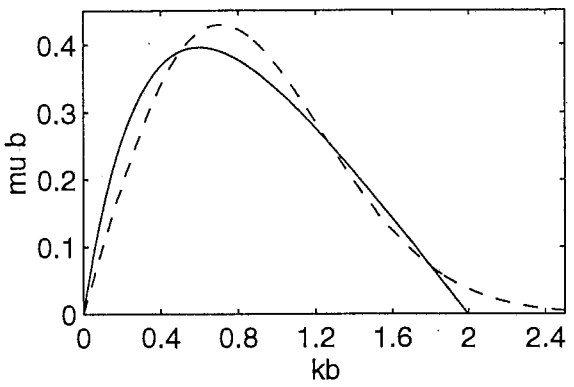

Figure 3: Amplification factor μ (bold line) and its approximation (dashed line) by an analytic function as functions of the frequency parameter kb. b is the half-thickness of the jet and $k = \omega/V_{\text{phase}}$, where ω is angular frequency.

As for the phase velocity V_{phase}, it is assumed to be proportional to $\omega^{1/2}$ or $\omega^{1/3}$ at the low frequency limit.[2] It is also about the same as one half of the jet velocity V_{jet} in the pipe sound frequency range.[8]

If we obtain an analytic time-domain representation of Eq. (9), it brings an enormous time reduction for the simulation. To this end, we substitute the analytical function,

$$\mu b = k b e^{-(kb)^2}, \tag{11}$$

for μ in Eq. (10) as an approximation. The dashed line in Fig. (3) depicts this function. To this same end, we assume that V_{jet} is a constant, independent of ω and equal to V_{phase}. As γ was introduced in the previous section, generality is not lost with this assumption.

With these procedures, the Fourier transformation of Eq. (9) becomes

$$G(t) = \epsilon(t)\,\epsilon(T-t) + \frac{1}{16\sqrt{2\pi}}\frac{T^2}{\tau^2}\frac{T-t}{\tau}e^{-\frac{1}{8}\left(\frac{T-t}{\tau}\right)^2}, \tag{12}$$

where $T = x/V_{\text{jet}}$ and $\tau = b/V_{\text{jet}}$. The function $\epsilon(t)$ in Eq. (12) is the step function defined by 1 for $t \geq 0$, otherwise 0.

With this kernel function $G(t)$, jet displacement $\xi(x,t)$ can be written as the following convolution integral:

$$\xi(x,t) = \alpha \int_0^\infty ds\, G(s) v(t-s). \tag{13}$$

Parameter α is newly introduced to adjust the amplitude of ξ. As $G(t)$ is localized, it is justified that the upper limit of the integral in Eq. (13) can be treated as $2T$ in the numerical calculation.

4.2 Acoustic particle velocity model

From the Fourier transformation of Eq. (2), a time-domain representation of this model can be obtained as

$$\xi(x,t) = \alpha T v(t-T) \tag{14}$$

with $T = x/V_{\text{jet}}$. As in Sec. 4.1, we introduced a parameter α to adjust the amplitude.

Lagrange differentiation of Eq. (14) indicates that volume element flowing together with the jet moves at a constant velocity in the direction of jet thickness. The velocity is equal to the acoustic particle velocity$\times\alpha$ at the moment the flow appears at the flue exit.

4.3 Pressure gradient model

In the original model, pressure gradient Δp is only a hypothetical quantity. This paper assumes that it is equal to $p/\Delta L$, where p is mouth pressure and ΔL is the end correction of the mouth. Introducing α as in the previous sections, we have

$$\xi(x,t) = \frac{\alpha}{\rho \Delta L}\int_0^T ds\, s\, p(t-s). \tag{15}$$

Equation (15) implies that a volume element with the jet moves with the acceleration of $\alpha p(t)/(\rho\Delta L)$ in the direction of jet thickness.

5 Simulation

5.1 Self-excited system

Self-excited oscillation can be described by mouth pressure p, acoustic volume flow U and jet volume flow $U_{\rm jet}$. Jet volume flow $U_{\rm jet}$ is a function of the jet displacement of the cut-up length $\xi(l)$ (Eq. (8)). The three variables p, U and $U_{\rm jet}$ are mutually related through the jet deflection model, resonance characteristic of the instrument and radiation characteristic of the mouth.

The volume flow rate U flowing into the instrument is given by the product of particle velocity v and mouth area Wl:

$$U(t) = -Wlv(t), \tag{16}$$

where the negative sign comes from the difference between defined directions of particle velocity v and volume flow rate U. The total volume flow $U^{\rm total}$ is

$$U^{\rm total}(t) = U(t) + U_{\rm jet}(t). \tag{17}$$

Resonance of an instrument is represented by input acoustic admittance $Y_\omega = U_\omega^{\rm total}/p_\omega$, which is the ratio of total volume flow $U_\omega^{\rm total}$ to mouth pressure p_ω. Using pressure reflection function $r(t)$ defined by the inverse Fourier transformation of the reflection coefficient

$$R_\omega = \frac{Y_0 - Y_\omega}{Y_0 + Y_\omega}, \tag{18}$$

we have the following time-domain representation:

$$Y_0\, p(t) = U^{\rm total}(t) + \int_0^\infty ds\, r(s)\Big(Y_0\, p(t-s) + U^{\rm total}(t-s)\Big), \tag{19}$$

where the characteristic acoustic admittance is $Y_0 = S_{\rm pipe}/(\rho c)$, with air density ρ, sound speed c and area of pipe $S_{\rm pipe}$.

Prior to the simulation, we calculated a reflection function from an acoustic admittance Y_ω of a cylindrical pipe, which has an area of $S_{\rm pipe} = 16{\rm cm}^2$ and a length of 44cm. These particular dimensions mimic those of the experimental E_4 organ pipe (except the foot) Fletcher[9] used for his experiments and analytic calculations. In the calculation of Y_ω, plain wave propagation is assumed and propagation loss in the pipe and radiation loss at the far end of the instrument are both considered.

The radiation characteristic at the mouth is represented by radiation impedance $Z_\omega^{\rm rad} = -p_\omega/U_\omega$. In the region of the pipe sound frequency, frequency parameter ka (k is the wave number and a is the characteristic length of the mouth) is small. Therefore, it is sufficient that $Z_\omega^{\rm rad}$ is considered as

$$Z_\omega^{\rm rad} = \frac{i\omega\rho\Delta L}{S_{\rm pipe}} \tag{20}$$

with end correction ΔL. Alternatively, we obtain the time-domain representation

$$\frac{dU(t)}{dt} = -\frac{S_{\rm pipe}}{\rho\Delta L}p(t). \tag{21}$$

In the simulation, ΔL is set to 5.9cm, which comes from Eq (17.5) in Ref. [1].

The time-domain simulation is carried out with the three equations: one of the three jet displacement models (13), (14) or (15), the feedback equation (19) and the radiation impedance (21).

5.2 Simulation results

In the simulation, the fundamental frequency and levels of harmonic components of the E_4 flue pipe are obtained as functions of blowing pressure p_0. Results of the negative acoustic displacement model, acoustic particle velocity model and gradient pressure model are presented in Figs. 4 (a), (b) and (c), respectively. The experimental result on the pipe with identical mouth dimensions is shown in Fig. 2 (b) in Ref. [9] (Fletcher).

In each simulation, mouth pressure p_0 is changed from 32Pa to 10kPa. As hysteresis is observed during the simulation, the pressure p_0 should be increased and decreased from the pressure range where the stablest

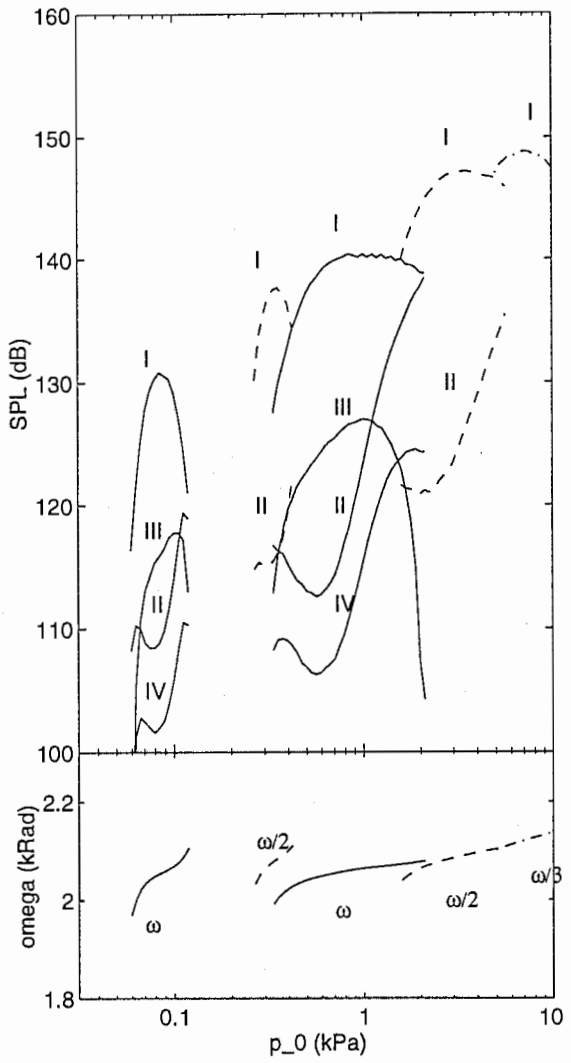

Figure 4(a): Negative acoustic displacement drive with $\gamma = 0.35$, $\alpha = 0.2$. Sound pressure levels (SPL) at the mouth and sound frequency ω (kRad) as functions of blowing pressure p_0 (kPa).

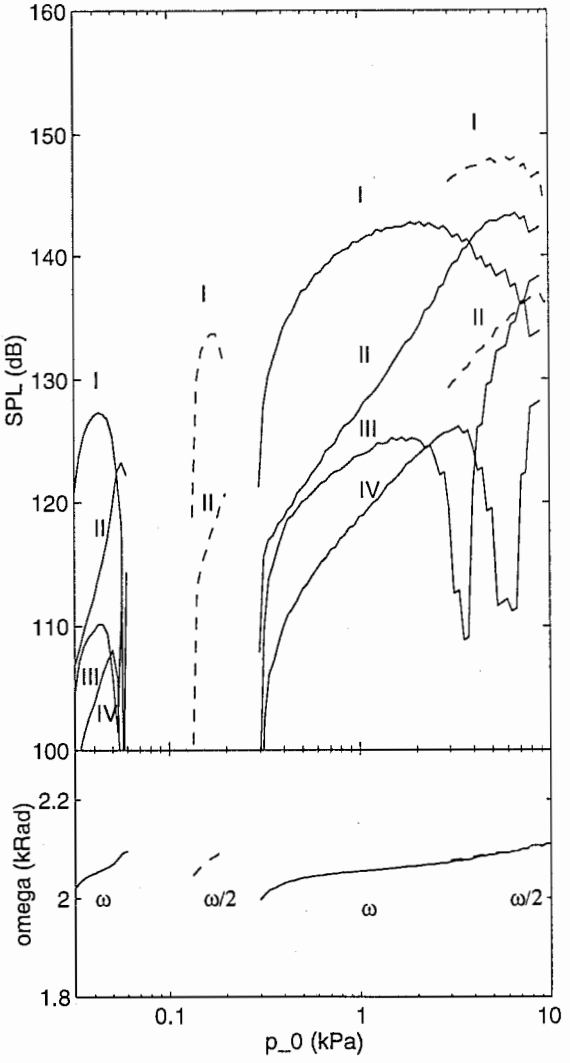

Figure 4(b): Acoustic velocity drive with $\gamma = 0.6$, $\alpha = 0.4$

oscillation is excited to obtain the whole self-excitation region. This is why overlapping of pressure regions for the regimes of oscillation occurs.

Dimensions of the mouth are fixed by the cut-up length $l = 10$mm, mouth width $W = 4$cm and flue slit thickness $h = 0.25$mm, which are identical to those in Ref. [9]. On the other hand, edge offset is estimated to be $h_{\text{off}} = 0.9$mm, and this is not explicitly described in the experiment. The jet spreading angle ϕ is set to 6.3° ($\tan\phi = 0.11$). This is the value obtained experimentally in Ref. [8].

The parameters γ and α introduced in the model formulation are determined in the preliminary simulation. As γ controls jet velocity V_{jet}, it changes the blowing pressure at which transitions among the oscillation modes occur. Therefore, γ is adjusted such that the transition between fundamental and second modes occurs near $p_0 = 2$kPa. Then, α is adjusted such that levels of harmonics of the fundamental mode oscillation have the same tendency as the experimental result. Table 1 lists the parameters set in each model.

In the simulations, no matter which model

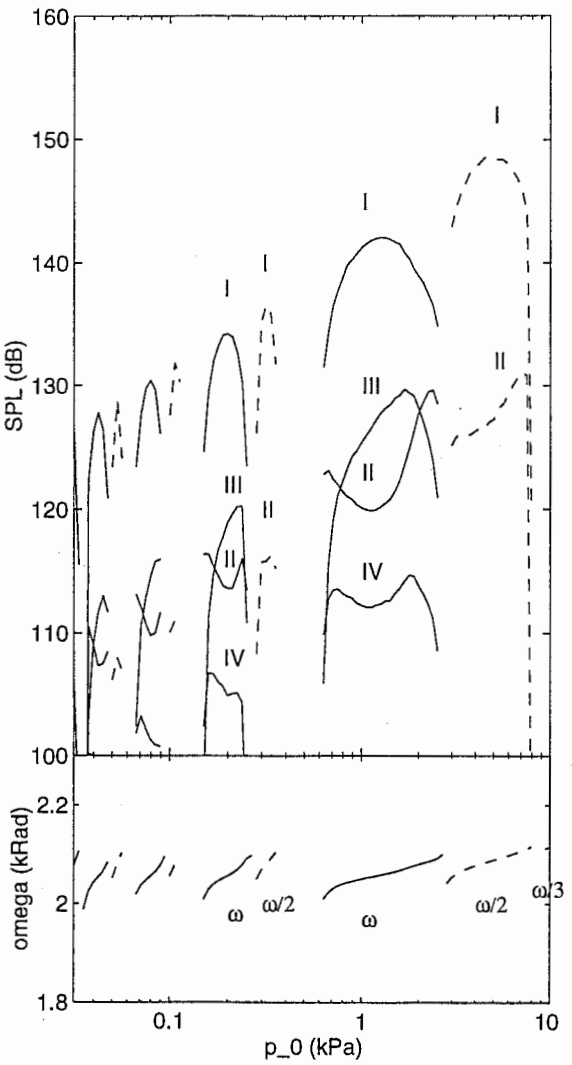

Figure 4(c): Pressure gradient drive with $\gamma = 0.2$, $\alpha = 0.42$

Table 1: Jet velocity parameter γ and jet deflection amplitude parameter α

	(a) X drive	(b) v drive	(c) Δp drive
γ	0.35	0.6	0.2
α	0.2	0.4	0.42

is used, oscillations in the fundamental and second resonance modes are generated. The fundamental frequency of the latter is about twice as much as that of the former. In the negative acoustic displacement model and the pressure gradient model, oscillation in the third mode (which has a frequency roughly three times) is also obtained.

It is also found that the underblow regime of oscillation (in which the traveling jet in the mouth has more than a 2π whole phase angle) appears when the blowing pressure is small. In this regime, oscillation in both fundamental and second modes are excited.

Fundamental frequency is increased as the blowing pressure rises, regardless of the regime of oscillation and oscillation mode. This is a characteristic found commonly in flue instruments.

Some differences among the jet displacement models appear in the levels of harmonics of oscillation. In the negative acoustic displacement model and pressure gradient models, odd harmonics (especially the third) of oscillation in the fundamental mode are enhanced. This phenomenon does not appear in the acoustic particle velocity model. In this model, the phenomenon of the third and fourth harmonics being suppressed at particular blowing pressures is observed. It is, currently, uncertain whether this phenomenon is specific to this model or depends on selection of simulation parameters. However, the cause should be clarified in a future simulation.

As compared with the experimental result (Fig. 2 (b) in [9]), the negative acoustic displacement model would be most favorable. This is because the particle velocity model cannot explain the odd harmonic dominance and the pressure gradient model has too many underblow regimes in the weak blowing pressure region. This is, however, a result of limited simulations in this paper. To obtain a more definite result, we probably need to carry out simulations with other mouth dimensions. At the same time, improvements in the simulation system such as accurate modeling of jet behavior, modeling of radiation from the mouth applicable even at a higher frequency and derivation of a minute pipe resonance characteristic are needed.

6 Conclusions

Time-domain representations of jet displacement models that have already been proposed in literature were obtained. Using the representations, a feedback equation for resonance of an instrument and radiation characteristic of the mouth, we carried out simulations. The fundamental frequency and levels of harmonics of the simulated oscillations were examined. As compared with the experimental result, we have discussed the performance of these models.

In the simulation, oscillation in the fundamental mode and other higher modes (overblows) were generated. Apart from the normal regime of oscillation, another regime called underblow was obtained in the weak blowing pressure range.

Although our simulation was limited to one configuration of the mouth, it gave the conclusion that the negative acoustic displacement model would be most favorable.

References

[1] N.H. Fletcher and T. Rossing, *The physics of musical instruments* (Springer-Verlag, New York, 1991) Chap. 16 426–466

[2] N.H. Fletcher and S. Thwaites, "Wave propagation on an acoustically perturbed jet", Acustica **42** 323–334 (1979)

[3] J.W. Coltman, "Jet drive mechanisms in edge tones and organ pipes", J. Acoust. Soc. Am. **60** 725–733 (1976)

[4] S. Yoshikawa and J. Saneyoshi, "Feedback excitation mechanism in organ pipes", J. Acoust. Soc. Jpn. **E1** 175–191 (1980)

[5] J.W. Coltman, "Jet behavior in the flute", J. Acoust. Soc. Am. **92** 74–83 (1992)

[6] P.A. Skordos and G.J. Gussman, "Comparison between subsonic flow simulation and physical measurements of flue pipes", in Proc. of the ISMA (1995) 79–85

[7] M.P. Verge, B. Fabre, W.E.A. Mahu, A. Hirschberg, R.R. van Hassel, A.P.J. Wijnands, J.J. de Vries and C.J. Hogendoorn, "Jet formation and jet velocity fluctuations in a flue organ pipe", J. Acoust. Soc. Am. **95** 1119–1132 (1994)

[8] S. Thwaites and N.H. Fletcher, "Wave propagation on turbulent jets: II. Growth", Acustica **51** 44–49 (1982)

[9] N.H. Fletcher, "Sound production by organ flue pipes", J. Acoust. Soc. Am. **60** 926–936 (1976)